J. Appl. Comput. Mech., 6(1) (2020) 112-124
DOI: 10.22055/JACM.2019.28242.1466

ISSN: 2383-4536
jacm.scu.ac.ir

M&MoCS

Shahid Chamran University of Ahvaz

Journal of Applied and Computational Mechanics

Research Paper

Upgrading the Seismic Capacity of Pile-Supported Wharfs Using Semi-Active Liquid Column Gas Damper

Reza Dezvareh

Assistant Professor, Faculty of Civil Engineering, Babol Noshirvani University of Technology
Shariati Av., Babol, Mazandaran, 47148 - 71167, Iran, Email: rdezvareh@nit.ac.ir

Received January 14 2019; Revised March 09 2019; Accepted for publication March 11 2019.
Corresponding author: Reza Dezvareh (rdezvareh@nit.ac.ir)

Abstract. One of the most important structures in the ports is the wharf. The most common one is the pile-supported wharf. This type of wharf is consisted of a number of piles and one deck which placed on the piles. In addition to the conventional loads that this structure should withstand, in seismic areas, pile-supported wharfs should have the necessary capacity and strength against seismic excitations. There are some approaches to increase the seismic capacity of the berth. One of these methods is to control the vibrations of the pile-supported wharf against earthquake loads using a damper. In this research, for the first time, a new semi-active damper called the semi active liquid column gas damper (SALCGD), was used to reduce the response of pile supported wharf under seismic loads. In the first step by applying different records of the earthquake, the most important parameter of this damper - the optimal opening ratio of the horizontal column- was obtained for this particular structure. In the following, the performances of this damper and its comparison with the tuned liquid column gas damper (TLCGD) were discussed. This study showed that the use of this semi-active damper (SALCGD) reduces the displacement of the pile-supported wharf by 35% and reduces the acceleration of the structure by 50% on average. In contrast, the passive damper (TLCGD) reduces the displacement of about 20 percent and the acceleration of about 30 percent. Therefore, it was observed that the semi-activation of the damper (SALCGD) had a significant improvement in its performance in controlling the vibrations of pile-supported wharf.

Keywords: Pile-Supported wharf; SALCGD; Seismic capacity; Vibration control.

1. Introduction

The Pile-Supported Wharf is one of the conventional coastal structures used for ship-berthing shipwrecking. This type of wharf includes a number of piles and a deck on it. In addition to the dead loads, the weight of the berthing equipment on them and the impact of the ship, these wharf should have the necessary resistance and strength against the earthquake force. Gerolymus et al. first used batter piles to provide the seismic capacity of the pile-supported wharf [1]. Then, Polous provided a new method for reducing the displacement of the wharf under the earthquake lateral load [2]. But as the cost of building and implementing of batter piles are high and due to the punching failure problem in their connections, Oyenuga et al. designed a new connection to reduce the punching failure problem [3]. Mageao and Chin also improved the seismic behavior of the pile-supported wharf by inventing a stone column [4]. In this research, we used a tuned damper to provide the seismic capacity of the pile-supported wharf and reduce the response of the pile-supported wharf under the earthquake load. Nowadays, the use of a variety of dampers to reduce the response of various structures or increase their load-carrying capacity under various dynamic loads such as earthquake, wave, wind, etc. have come to the focus of attention. In general, the control of the structure vibrations is divided into three

Published online: July 11 2019

categories: passive (non-active), active and semi-active. The passive control implies that the devices and equipment used have a fixed and predetermined profiles and behaviors. In this regard, Soong and Dargush have presented various methods [5]. Investigations and using of TMD have continued in recent years, as an example, Tributsch and Adam have estimated the impact of this damper in seismic excitations [6]. Domenico and Ricciardi have also been working on the design of this damper in base isolated systems [7, 8]. Also, Elias et al. controlled the vibration of the chimney under the wind loads by multiple TMD [9].

In active control, the structure is equipped with a damper that can intelligently apply a specific force to neutralize the external forces applied to the structure. The dampers such as active tendons and active mass dampers are some examples in this area that Nishimura et al. presented an active control strategy for the tuned mass damper [10]. Active vibration control is a technique for reducing unwanted vibration by using some kinds of sensor to measure the motion, force, acceleration and other parameters. So this technique is more difficult than passive control in the vibration reduction of systems. The idea of semi-active control has been presented to simultaneously use the passive and active control features. This method does not require a large energy source and a small energy source such as a battery is enough to change the specifications of a damper. For example, in the case of a semi-active viscous damper, Suleman et al. have opened and closed the damper valve for semi-active control of the structure by using a battery. Hence, semi-active control is superior to active control in terms of cost and reliability [11]. The tuned fluid column damper is one of the types of tuned dampers, which consists of a U-shaped tube with a fixed cross-section filled with the fluid. The vibration energy is transferred from the structure to the fluid inside the TLCD and dissipated by the fluid gravity recursive force and hydrodynamic head loss mechanisms such as friction, orifice, and elbow. Regarding this damper, extensive research has been done on its optimal design [12], its performance evaluation [13] and its combining with the TMD [14]. As stated by Hitchcock et al., the idea of energy transfer to fluid is not limited to stable structures and has been investigated in the past to control the vibrations of ships and satellites [15]. Over time, its improved version called the Liquid Column Vibration Absorber (LCVA) was introduced. The LCVAs are like Tuned Liquid Column Dampers (TLCDs) with the difference that the cross-sections of the vertical columns and horizontal columns in the LCVAs are not the same [16]. At first glance, it may not seem a significant difference, but it greatly improves the performance of the damper. This is a passive type damper; whose semi-active prototype was provided by Yalla et al. [17]. Moreover, Hemmati and Oterkus have studied a model for offshore wind turbine systems equipped with a semi-active time-variant tuned mass damper [18]. Further on Hemmati et al. have used combination of TMD and TLCD in offshore wind turbine [19]. Also, a new example of TLCDs, known as the Tuned Liquid-Gas Column Damper (TLCGD), has been presented by Hochrainer and Ziegler [20], which is exactly the same as the LCVA with the difference that the pressurized air is in the vertical columns above the fluid level, and in fact, the vertical columns are enclosed. This type of damper, of passive type, was later evaluated by Dezvareh et al. [21] and Bargi et al. [22] in offshore wind turbines and its various parameters were optimized under wave and wind loading as well as earthquake force. With regard to the above mentioned issues and the advantages of the tuned liquid-gas column damper (TLCGD) as well as the better performance in the semi-active control method, we studied the Semi-Active Liquid Column Gas Damper (SALCGD) in this research for the first time and its effect on reducing the responses of the pile-supported wharf under earthquake loading was evaluated.

2. Introducing Semi-Active Liquid Column Gas Damper (SALCGD)

The SALCGD is actually based on the passive tuned liquid column gas damper (TLCGD). Its difference is to control the applied force by placing a valve in the orifice and its opening and closing based on the external force involved. The fluid flow equation inside the TLCGD can be obtained through various methods. Consider a TLCGD in accordance with Fig. 1 where y represents the liquid level changes in the vertical column and x represents the displacement in the horizontal column. Also, b and h are respectively the length of the liquid in the horizontal and vertical columns. As a result, A_h and A_b are the cross-sections of vertical and horizontal columns. In this damper, h_a represents a length of the vertical column that is filled with a gas at the initial pressure of P_0. This gas is located in the vertical column and on the liquid.

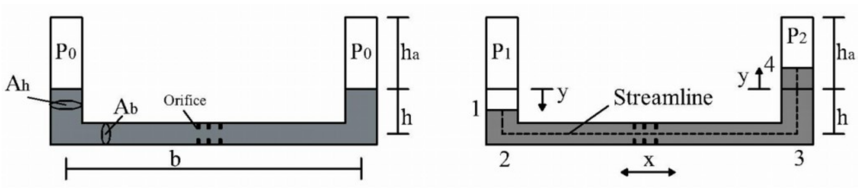

Fig. 1. Movement of the TLCGD under the stimulation of the base x and the relevant parameters

Based on previous researches and using the Newton's second law, this equation of motion has been obtained in accordance with Eq. (1) [21].

$$\ddot{y}+\delta_L\left|\dot{y}\right|\dot{y}+\omega_A^2 y=-k_1\ddot{x} \tag{1}$$

In this equation:

$$\omega_A^2 = \frac{2g(1+{}^{nP_0}\!/\!{}_{\rho g h_a})}{2h+b\lambda}, k_1 = \frac{b}{2h+b\lambda} \tag{2}$$

$$\delta_L = \frac{1}{2(2h+b\lambda)}\left\{K_{el}(1+\lambda^2)+N_b K_{or}\lambda^2+N_h K_{or}+\frac{8fh}{D_h}+\frac{4fb}{D_b}\lambda^2\right\} \tag{3}$$

In the above equations, ω_A and δ_L, respectively, are called the TLCGD frequency and head loss coefficient and λ is the ratio of the surface equal to the ratio of the cross section of the vertical column to the horizontal column. In these two above equations, K_{el} and K_{or}, respectively, are the coefficients of resistance for the elbow, the joint site of the horizontal column to the vertical column, and the orifice, while N_b and N_h are respectively the number of the orifices of the orifice planes in the horizontal and vertical columns (sum of the two vertical columns). D_h and D_b are the diameters of the vertical and horizontal columns, respectively and " f " is the Darcy's friction coefficient, which values depend on the material of the inner wall of the TLCGD columns. The important point about the TLCGD is that the fluid movement should be such that no gas enters the fluid at all. In other words, the mixing of gas and fluid is not allowed and should be avoided. To this end, according to Linder-Sylvester and Schneider studies, the necessary condition is that the fluid velocity inside the vertical column would be smaller than 10 m/s ($|\dot{y}| \le 10\ m/s$) [23].

The above are brief explanations and governing equations for the TLCGD. The hardness control algorithm by the bang-bang (on/off) method is used to semi-activate this damper. In this control algorithm, the damping coefficient is adjusted as such that the damper controlling force changes suddenly depending on the displacement direction and the speed of the damper [24]. In other words, if the speed and displacement of the damper have the same signs, the damping coefficient of the damper will be equal to its maximum value; otherwise, this coefficient is equal to its minimum value. The above algorithm can be expressed mathematically by the following equation:

$$c = c_{\max}H(u,\dot{u}) + c_{\min}H(-u,\dot{u}) \tag{4}$$

In the above equation, u is the displacement of the damper and the point operator represents the derivative in terms of time. Also, H is the Heaviside function, which will be 1 for positive values and 0 for negative values, respectively. The variable damping coefficient as well as the maximum and minimum damping values of the damper are shown with c, $c_{\max}$, and $c_{\min}$, respectively. For adapting this algorithm and its use in the TLCGD, since the damping in this type of damper is directly related to the hydraulic head loss factor of δ_L, the hydraulic head loss factor is placed in Eq. (4) instead of the damping coefficient. In this case, according to Eq. (1), the displacement u and the velocity $\dot{u}$ also turn into the displacement x and the fluid velocity $\dot{x}$ inside the damper in the horizontal direction, respectively. In other words, the equation of motion of the SALCGD is as the same as the equation of motion of TLCGD (Eq. (1)) with the difference that the value of the hydraulic loss factor is not constant in the SALCGD. Thus, depending on the external force exerted on the system and based on the Bang-Bang algorithm, the hydraulic loss coefficient can take its minimum or maximum value at any time step, which can be done by opening and closing the valve:

$$\delta_L = \delta_{L_{\max}}H(x,\dot{x}) + \delta_{L_{\min}}H(-x,\dot{x}) \tag{5}$$

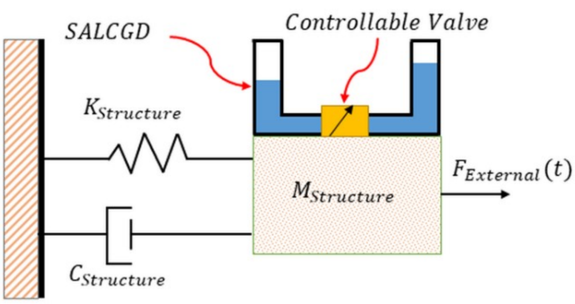

Fig. 2. SALCGD system and the structure

A controlling valve is required to change the value of the hydraulic loss coefficient according to Fig. 2. As described, in the semi-active control mode, the controlling valve is set in two open and closed modes, or in other words, off and on modes. In the SALCGD, if the control valve is completely open, the hydraulic loss coefficient is considered to be 0.5 according to Mousavi et al. [25]. In fact, this figure is the minimum hydraulic loss coefficient ($\delta_{L_{\min}}$) at the SALCGD of the present study. The amount of hydraulic loss of the SALCGD increases with the valve closure. According to Wu research, the relationship between the amount of the hydraulic loss coefficient and the valve closure percentage is defined as below [26].

$$\delta_L = (-0.6\varphi + 2.1\varphi^{0.1})^{1.6}(1-\varphi)^{-2.0}, \varphi > 0 \tag{6}$$

In the above equation, φ is the ratio of the valve closure to the total valve. As can be seen, this equation does not apply to the case where the valve is completely open and the value of the hydraulic loss is equal to 0.5 in the completely open mode. According to the Eq. (6), various ratios of φ are examined in this study to determine the optimal value of the valve closure and calculate the hydraulic loss coefficient in this case, which is equal to the maximum hydraulic loss coefficient ($\delta_{L_{\max}}$).

3. The Controlling Effect of the SALCGD on the Structure

Energy absorbers reduce the response of the structure under dynamic loads by absorbing some of the energy entering the structure. The above explanation is based on energy, while it can also be explained based on the force. The energy absorbers have a vibrational mass called the secondary mass. There are many studies dealing with energy-based design strategies of vibration absorbers and viscous dampers [27-30]. With its vibration, the secondary mass applies force to the main structure. If the energy absorber frequency is set, this force acts in such a way to reduce the response of the main structure. Simply put, when the main structure moves to the right, this force enter the main structure in the left direction, and vice versa, when the main structure moves to the left, the force will be applied to the right. The above force is the result of two forces:

- The force generated by the total inertia of SALCGD due to the absolute acceleration of the structure (The acceleration of a point of the structure where the SALCGD is installed)
- The force induced by the inertia of fluid flow inside the horizontal column of the SALCGD

In the semi-active control, the force caused by inertia of the fluid movement is controlled by opening and closing the valve in such a way to induce the greatest reduction effect on the structure response. In other words, the advantage of SALCGD over TLCGD is that the controlling power is not constant at all-time steps but its value changes under different conditions to control the structure.

It should be noted that the motion of the fluid in the horizontal column is only raised in the case of the second force since the movement of fluid in the vertical columns causes the application of vertical forces, which do not affect the studied lateral response of the structure. If the first force is represented by F_1 and the second force with F_2, we would have:

$$F_1 = m_f\ddot{x} \quad , \quad F_2 = \rho B A_b \lambda \ddot{y} = \rho B A_h \ddot{y} \tag{7}$$

The values of these two forces are such that their outcome leads to reduced responses. With the algebraic summation of the two above forces, the force applied by the SALCGD to the structure is obtained as follows:

$$F = m_f(\ddot{x} + \bar{k}\ddot{y}) \quad , \quad \bar{k} = \frac{B}{2h + B/\lambda} \tag{8}$$

In the above equations, the fluid weight inside the SALCGD is shown with m_f; also, x represents the local displacement of the structure where the damper is located and the above force is applied at the same point to the main structure. It should be noted that usually the mass of the damper tubes is ignored or their mass is considered in the mass of the main structure.

4. Introduction of the Pile-Supported Wharf

As shown in Fig. 3, the pile-supported wharf can be considered as a system of a single degree of freedom. Nowadays, as there is a need for new pile-supported wharfs with longer piles, and thus, larger periods due to the increase in the capacity and size of ships and the depth of their drafts, therefore, we considered the main period of this structure from 0.4 to 1.4 seconds in this study to examine the pile-supported wharfs in different depths. The masses of these docks were 200 tons.

In Fig. 3, steel piles have 1 m diameter and 10 mm thickness. These piles are assumed to support the wharf deck. Spacing between piles is 5 m along the shoreline. Also, the concrete slab of wharf deck has 40 m length perpendicular to the shoreline, 60 m width along the shoreline and 0.4 m thickness. And inherent damping ratio of its first mode is considered 5%.

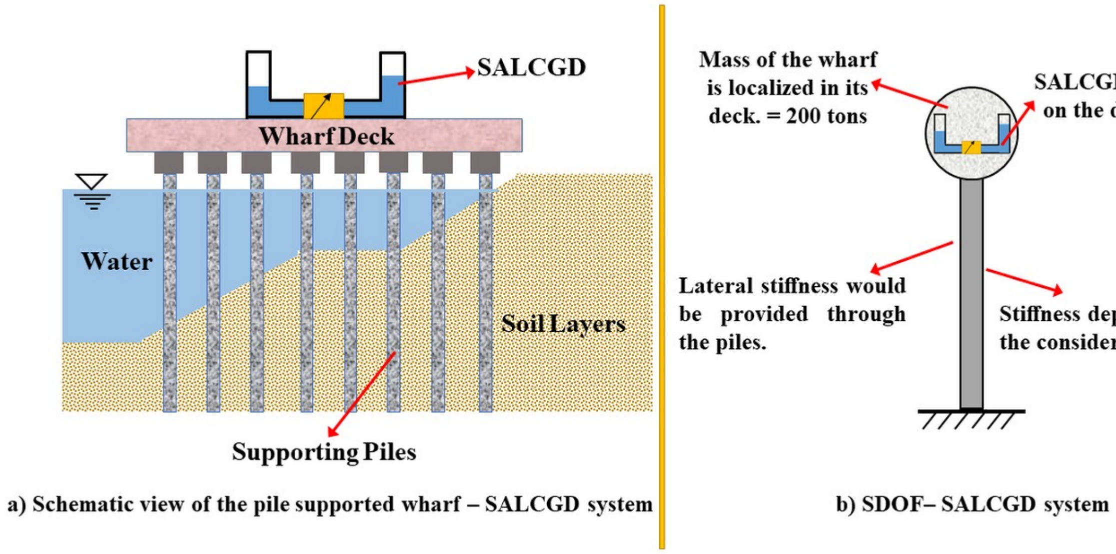

Fig. 3. The pile-supported wharf with SALCGD system

Since, at the time of the earthquake, one can assume that the displacement above the retaining wall is equal to the movement of the bottom of the berth, i.e., the same level of the sea bed, then, we did not consider a degree of freedom of the retaining wall in the model in this research to evaluate the different retaining walls with different dynamic behaviors. However, its effects were regarded somehow due to this wide range of periodicity of the structure although this assumption has been reasonable in the laboratory observations of Towhata et al. [31]. The structure of the wharf is in interaction with the soil. So layering and soil type affect its behavior. This effect increases or decreases in the period of the structure. Therefore, since the purpose of the present research is parametric studies, rather than a case study, different types of wharfs with different periods are considered to take into account the effects of different types of soil which interaction with structure.

Based on most maritime regulations, including the OCDI code, the pile-supported wharf structure should remain elastic under extreme earthquake. Therefore, it was assumed in the study that the structure of a degree of freedom represents the pile-supported wharf in the elastic region [32].

5. The pile-Supported Wharf and the SALCGD System

5.1 Equation governing the system

Using the obtained equations, we can easily determine the equation of motion of the pile-supported wharf - SALCGD system. In fact, it is only sufficient to add a vector of force corresponding to the damper force to the dynamical equation of the pile-supported wharf according to Eq. (8) (Fig. 3).

$$F_{Inertia} + F_{Damping} + F_{Elastic} = F_{seismic} + F_{SALCGD} \tag{9}$$

One can conclude from the equations of the SALCGD and also the Eq. (9) that the value of the acceleration of the fluid within the SALCGD is required to solve them. On the other hand, the values of displacement, velocity and acceleration of the pile-supported wharf are required to obtain these parameters. Therefore, the equations of the pile-supported wharf - damper system are coupled with each other. Thus, the Simulink software, one of the lateral features of MATLAB software was used to solve these nonlinear and coupled differential equations. In Simulink, the coupled equations can be solved by using the definition of the loop [33].

5.2 Simulink model

The general model of the Simulink made based on the equation of motion of the pile-supported wharf - damper system according to Eq. (9) is shown in Fig. 4. As can be seen, the Simulink model is consisted of three blocks of the main structure, the SALCGD and the semi-active control that are interconnected properly in accordance with the ruling relationships. The direct input of this model is also the time history of the earthquake record acceleration, which provides the earthquake force after being multiplied by the mass of the model. The numerical algorithm which is used in Simulink model, is Runge–Kutta method. In numerical analysis, the Runge–Kutta methods are a family of implicit and explicit iterative methods, which include the well-known routine called the Euler Method, used in temporal discretization for the approximate solutions of ordinary differential equations. These methods were developed around 1900 by the German mathematicians Carl Runge and Martin Kutta [34].

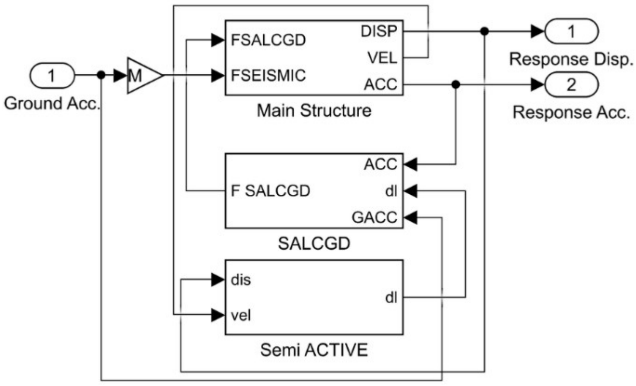

Fig. 4. The overview of modeling in the Simulink

In Fig. 5, the block related to the model of the main structure of the pile-supported wharf - damper system is presented. In this block, according to Eq. (9), two external forces of the earthquake and the SALCGD force, which is calculated from the block of the damper, were considered as the inputs of this block. Also, three internal inertia forces of inertia, damping, and elasticity were calculated respectively through multiplying the values of mass, damping and stiffness (hardness) by acceleration, velocity, and the displacement of the structure. The structure response values (acceleration, velocity, and displacement) were obtained as the output of this analysis.

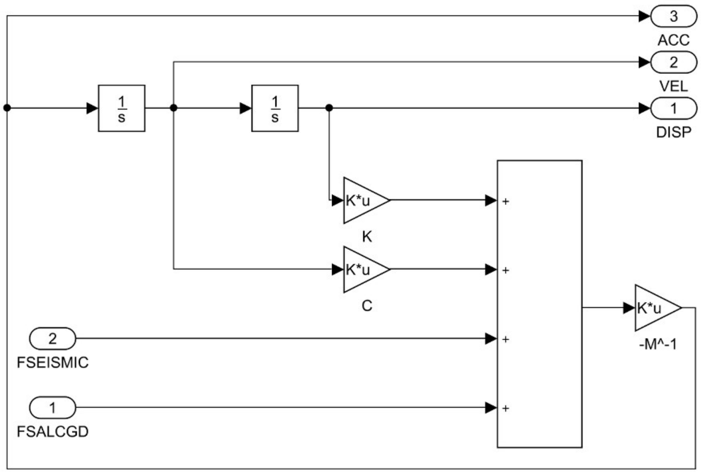

Fig. 5. The main block of the equation of motion of the structure – damper

In Fig. 6, details of the SALCGD block are provided. Based on the governing equations for SALCGD, the acceleration of the liquid in the vertical column of the damper is calculated from the acceleration of the structure in a level that the damper is placed. Therefore, in this figure, the acceleration of the structure at the level of the damper as input is combined with the acceleration of the fluid in the vertical column of the damper obtained from Eq. (1) to calculate the damper force in accordance with Eq. (8). The inputs of this block are the acceleration of the structure, the earthquake acceleration and the hydraulic loss coefficient obtained from the semi-active control block and its output is the controlling force of the SALCGD.

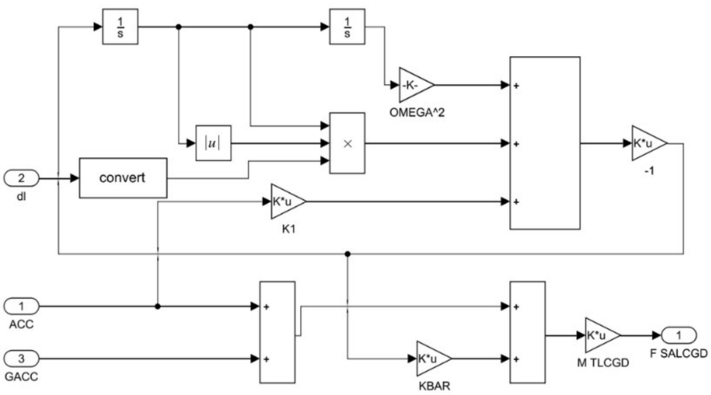

Fig. 6. Block related to the equation of motion of the damper

Fig. 7 shows the block related to the semi-active damper control. This block is based on the Bang-Bang algorithm and Eq. (5). Thus, at each time step, the displacement and velocity of the structure are entered as input to this block to determine whether to consider the maximum or the minimum of the hydraulic loss coefficient at that time step based on their sign according to Heaviside function. In other words, this block specifies that the valve would be fully opened or somewhat closed at each time step. In fact, the small energy source responsible for opening and closing the valve takes command from this block.

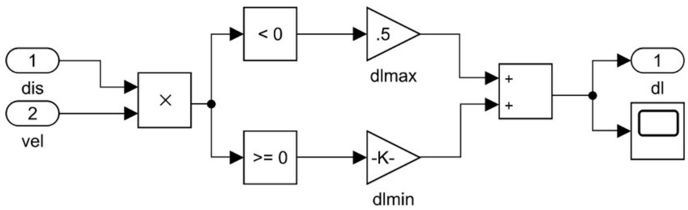

Fig. 7. The block related to semi-active damper control

6. Parametric Studies

According to what mentioned earlier and using the Simulink model presented in the previous section, the parametric studies were done on the damper specifications and its performance in reducing the response of the pile-supported wharf under the impact of the earthquake force to achieve the research objectives after describing the model specifications and the considered loads in this section. Since the important issue in the tuned dampers is to optimize its specifications to achieve the best performance and the maximum reduction in the structure response and as it is the first time that the SALCGD is being evaluated, the mentioned parametric studies were provided with a SALCGD parameters optimization approach.

Since this study attempts to investigate a semi-active damper (SALCGD) for the first time and its effects on the structure, the main focus is on the main parameter for its semi-activation, the blocking ratio. And other design parameters of damper, is intended as a passive damper (TLCGD).

6.1 Specifications of the pile-supported wharf

As shown in Section 4, six different types of berths were presented to consider different types of the pile-supported wharfs with different depths of the draft, which natural period varies from 0.4 to 1.4. Also, the intrinsic damping coefficient of these models is equal to 5% and their total mass was considered to be identically 200 tons. Using the equations presented in Chopra [35], the characteristics of these models, including their hardness and damping values were calculated in accordance with Table 1.

Table 1. The specifications of different types of the pile-supported wharfs

Type	T Period (s)	Angular Frequency	K Stiffness	C damping
Type 1	0.4	15.707963	49348022	314159.3
Type 2	0.6	10.471976	21932454	209439.5
Type 3	0.8	7.8539816	12337006	157079.6
Type 4	1	6.2831853	7895684	125663.7
Type 5	1.2	5.2359878	5483114	104719.8
Type 6	1.4	4.4879895	4028410	89759.79

6.2 Specifications of SALCGD

Optimization of damper parameters in a particular structure and under specific loading is one of the traditional studies conducted on various types of tuned dampers. Since the SALCGD has not been embedded in any structure and its parameters have not been optimized for earthquake loading, in the first step, we needed to optimize the parameters of this damper in the model. However, according to previous research, especially the studies by Dezvareh et al. [21] on the passive TLCGD, and in view of the similarities of the TLCGD and SALCGD dampers, in this study, we considered the common parameters of these two dampers such as the ratio of the damper mass to the mass of the structure ($\mu = m_{SALCGD}/M_{structure}$) and the ratio of the damper frequency to the natural frequency of the structure ($\alpha = \omega_{SALCGD}/\omega_{structure}$) to be the same. Thus, we focused the research on optimizing and obtaining the best value for the parameter of the maximum hydraulic loss factor ($\delta_{L_{\max}}$) or, in other words, the best value for the ratio of the valve closure to the total valve (φ).

According to the above explanations, since the main objective is to examine the blocking ratio, other damper parameters are considered based on the research done on the TLCGD. Therefore, in Table 2, the value of the ratio of the frequency (α) and the ratio of the mass (μ) is considered in accordance with the optimum value obtained in researches [21] and

[22]. Also, considering the dimensions of the structure, the length of the horizontal column (b) is 16 m, the length of the vertical column (h) is 1.5012 m and the cross-sectional ratio (λ) is 0.5, which leads to the calculation of the parameters k_1 and $\bar{k}$ in the table 2.

Also, based on Eq. (6) for different percentages of valve opening, the maximum hydraulic loss coefficient was calculated in accordance with Table 3. Then, an analysis was performed for each to obtain its optimal value.

Table 2. The SALCGD specifications

Parameter	value
k_1	1.4545
$\bar{k}$	0.457
μ	0.1
α	0.85
$\delta_{L_{min}}$	0.5
$\delta_{L_{max}}$	variable

Table 3. The values of the hydraulic loss coefficient according to the valve closing rate

φ	0.1	0.2	0.3	0.4	0.5	0.6	0.7	0.8
δ_L	2.640	3.542	4.688	6.347	8.994	13.730	23.720	51.641

6.2 Selection of earthquake records

According to Table 4, 20 earthquake records were selected from the Peer database [36] to evaluate the performance of the SALCGD and obtain the appropriate amount of the valve closure.

All of these records were scaled using the method presented in ASCE7 [37]. The return period intended for the earthquake hazard level was 475 years (10%, 50 years old) and the sea bed soil was chosen of the stiff type with a shear wave velocity of 350 m/s.

Table 4. The considered earthquakes

NO	Earthquake	Station Name	Un-scaled PGA(g)	Duration (s)
1	Tabas, Iran 1978/09/16	9101 Tabas	0.852	32
2	Northridge 1994/01/17 12:31	24278 Castaic - Old Ridge Route	0.568	40
3	Parkfield 1966/06/28 04:26	1014 Cholame #5	0.442	44
4	Chi-Chi, Taiwan 1999/09/20	CHY101	0.44	90
5	Friuli, Italy 1976/05/06 20:00	8012 Tolmezzo	0.351	36
6	Imperial Valley 1940/05/19 04:37	117 El Centro Array #9	0.313	40
7	Landers 1992/06/28 11:58	22170 Joshua Tree	0.284	44
8	Duzce, Turkey 1999/11/12	1062 Lamont 1062	0.257	42
9	Trinidad offshore 1983/08/24 13:36	1498 Rio Dell Overpass, E Ground	0.194	22
10	San Fernando 1971/02/09 14:00	126 Lake Hughes #4	0.192	36
11	Kern County 1952/07/21 11:53	1095 Taft Lincoln School	0.178	54
12	Cape Mendocino 1992/04/25 18:06	89509 Eureka - Myrtle & West	0.178	44
13	Loma Prieta 1989/10/18 00:05	58393 APEEL 2E Hayward Muir Sch	0.171	40
14	Kocaeli, Turkey 1999/08/17	Atakoy	0.164	130
15	Lytle Creek 1970/09/12 14:30	620 Devils Canyon	0.151	14
16	Kobe 1995/01/16 20:46	0 HIK	0.148	78
17	Borrego Mtn 1968/04/09 02:30	117 El Centro Array #9	0.13	40
18	San Francisco 1957/03/22 19:44	1117 Golden Gate Park	0.112	40
19	Aqaba 1995/11/22 06:16	Eilat	0.097	60
20	Taiwan SMART1(25) 1983/09/21	33 SMART1 E02	0.022	14

6.3 Calculating the optimal valve closure rate

The pile-supported wharfs of the previous section were analyzed under the 20 earthquake records of Table 4 in two with and without damper modes to obtain the optimal valve closure rate, in other words, the optimum value of the maximum hydraulic loss coefficient. Since the maximum value alone is not a suitable criterion for assessing the function of the damper in the analysis of the time history, as with other research in the area of structure vibrations control, the standard deviation of the responses was also considered as a measure of the damper performance in this study in addition to the maximum value of the structure displacement, which results are as shown in Fig. 8.

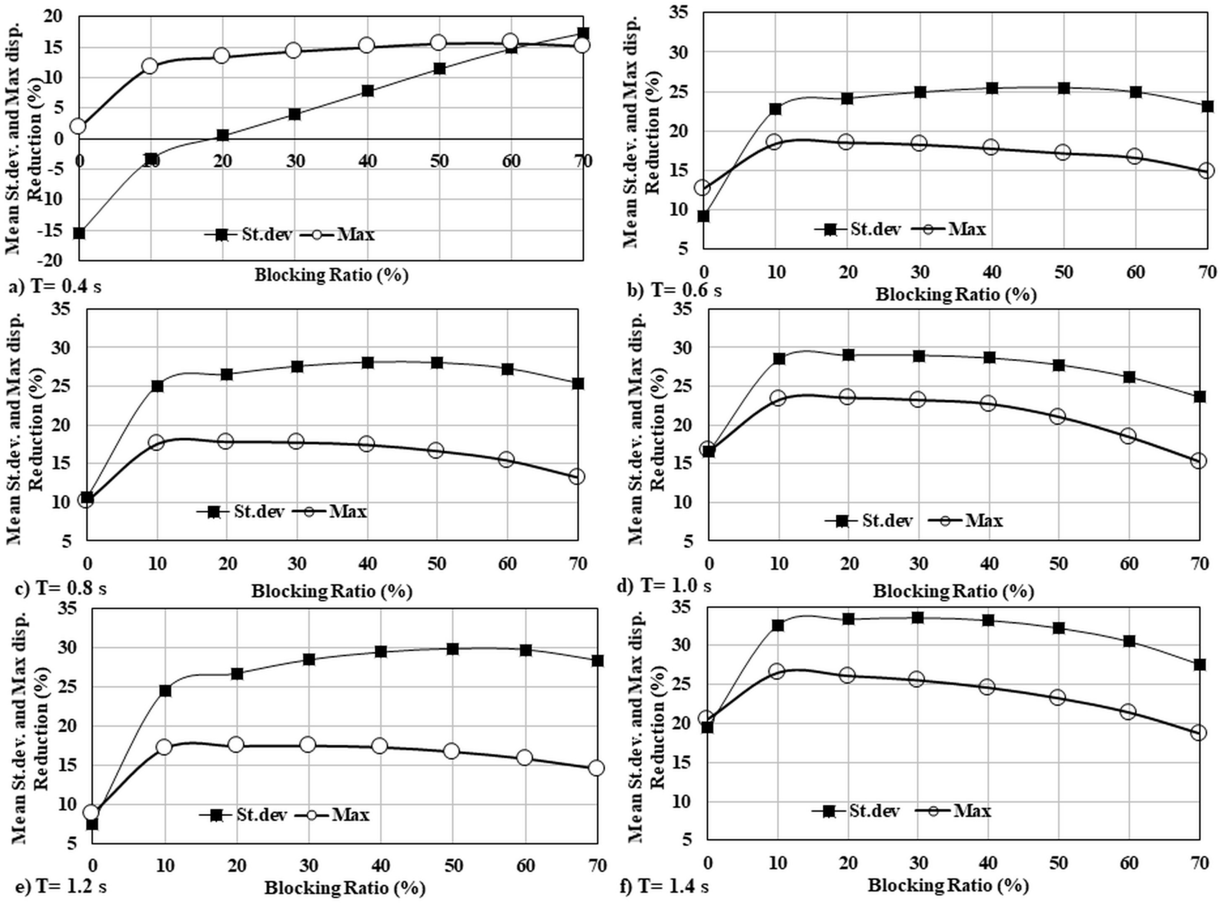

Fig. 8. The mean reduction of standard deviation and the maximum displacement of structure deck depending on different percentages of the valve closure

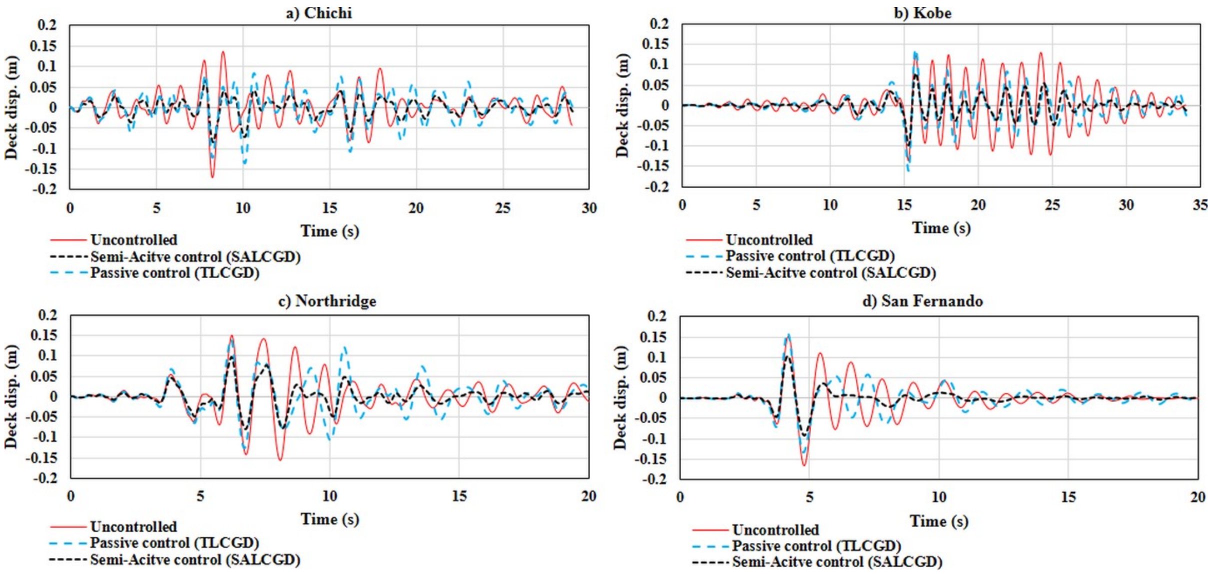

Fig. 8. Time history diagram of the displacement of the deck of the structure in three modes of without damper, with a passive damper and with a semi-active damper for various earthquakes

The above figure diagrams are basically the mean of the pile-supported wharfs analysis results under the twenty seismic records. In other words, each point on each of the graphs is the result of twenty analyses. Thus, 1080 different analyses were done in the Simulink to examine the damper function and find the best valve closure rate. As can be seen, the horizontal axis shows the amounts of different closures and the vertical axis is related to the percentage reduction of the two maximum values and the standard deviation of the wharf displacement in the case of using the SALCGD compared to the mode without the damper. It should be noted that the values corresponding to the closure of zero are in fact a state in which the valve is completely open and the maximum hydraulic loss coefficient and minimum hydraulic loss coefficient are the same. In other words, this point is related to the operation of a passive TLCGD damper. Therefore, the results well illustrate the advantages of the semi-active SALCGD compared to the passive TLCGD. For example, in the pile-supported wharf type 6 with a natural period of 1.4 seconds, the use of passive TLCGD only reduces 20% of responses, while using the SALCGD decreases the responses rate in the corresponding state with the best closure by about 35%.

The diagrams in Fig. 8 also show that by increasing the period of the wharf, and in other words, by increasing the length of the piles of the pile-supported wharf, the performance of the damper improves. This is highly optimal due to what described about the use of docks with longer piles and higher draft depths.

According to the above figure, the best blocking ratio seems to be 30% or 40% for the SALCGD. According to Table 3, the hydraulic coefficient was obtained about 5.

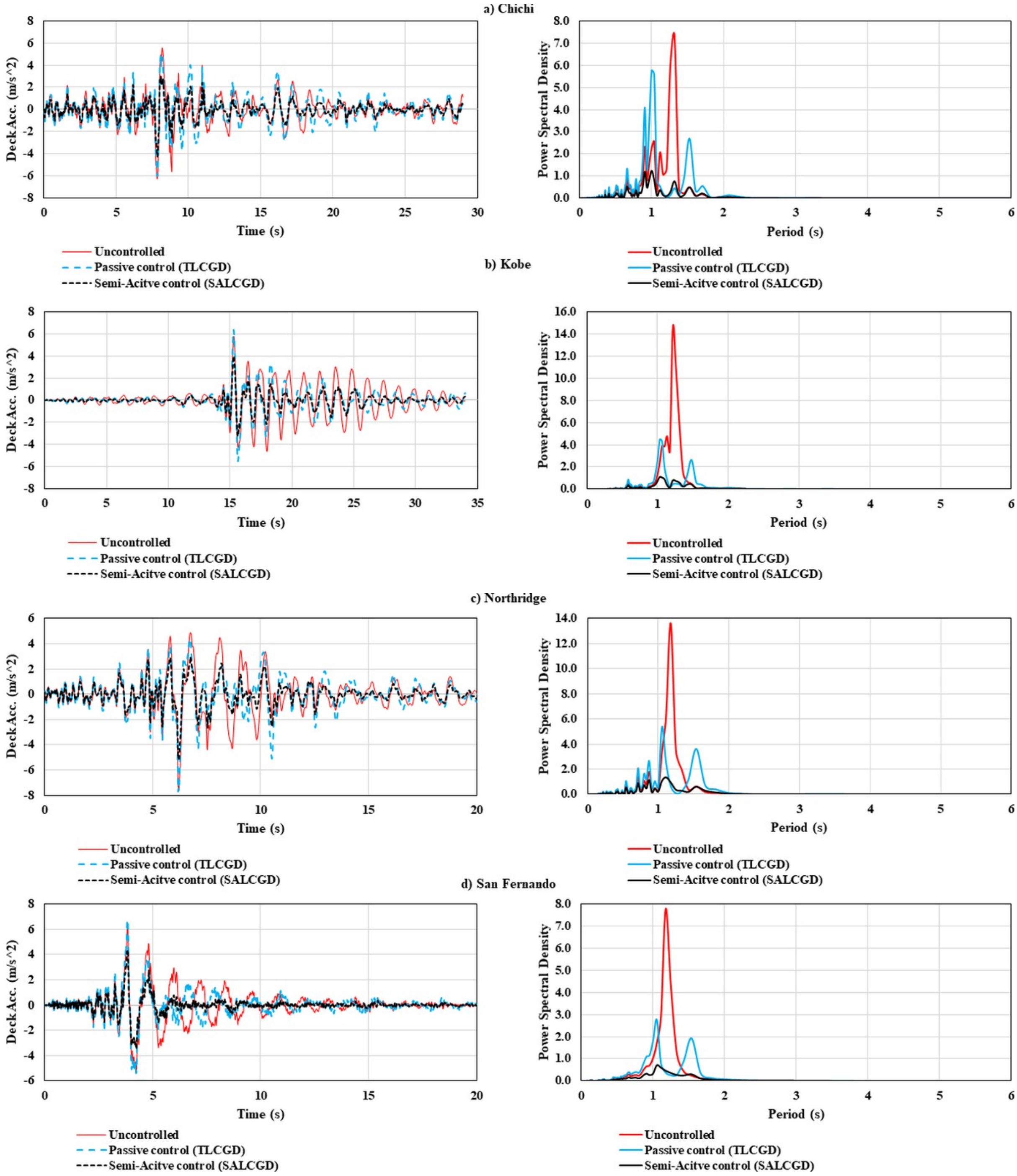

Fig. 9. Left: The time history diagram of the acceleration of the structure. Right: Power Spectral Density (PSD) Chart of the acceleration of the structure in three modes without a damper, with a passive damper and with a semi-active damper for various earthquakes

6.4 Assessment of the dynamic response of the pile-supported wharf with SALCGD

For more accurate analysis of the performance of the damper on the pile-supported wharf, the time history of the displacement of the wharf deck type 4 were provided in four famous earthquakes in Fig. 9. In this figure, the pile-supported wharf responses were compared in three uncontrolled (without a damper), controlled by a passive TLCGD, and controlled by a semi-active SALCGD states.The diagrams in this figure indicate that the SALCGD, shows a proper performance in the first seconds of the earthquake stimulation due to its semi-active nature. In other words, the problem with the passive TLCGD and other tuned passive mass dampers was that the damper is still sleep literally in the first seconds of dynamic stimulation and has a neutral performance in reducing responses, which is less common in the SALCGD.

Also, the results of the acceleration of the wharf under the four earthquake records were compared in two time histories and frequency areas (power spectral density) as follows to examine the performance of the damper in reducing the acceleration of the wharf, and consequently, reducing the shear forces.

The diagrams on the left in Fig. 10 show well that the performance of the semi-active SALCGD is also very effective and considerable in reducing the acceleration response of the structure so that the use of SALCGD reduces the response of the accelerated structure to about 50% compared to the uncontrolled mode and about 30% than to the passive control mode by the TLCGD. The diagrams on the right of this figure that compare the responses in the frequency space and is in fact the power spectral density (PSD) of the acceleration response of the structure, indicate the proper function of the SALCGD. It is also seen in these diagrams that by adding the damper to the structure, the corresponding period with the largest structure response is somewhat reduced, which suggests the validity of the performance of the structure-damper interaction model since with the addition of a damper to the system, the natural period of the structure is changed. Thus, the structure response is not maximized in the previous period anymore. In fact, a shift is created in the period corresponding to the maximum response of the structure according to the diagrams of Fig. 9.

The stroke is due to the relative displacement of the TMD to the primary structure (Define v_s, the PTMD displacement relative to the i_{th} floor, as the PTMD's stroke) [38]. This is not the case in the SALCGD because this damper is rigidly connected to the primary structure and the relative displacement of the primary structure and the secondary structure is zero. However, what should be considered in this damper, which is similar to the stroke of the TMD, is the displacement of the fluid in the vertical column (y), which dictates the total height of the vertical column ($h+h_a$). Therefore, in this study, the height of the fluid in the vertical column (h) is considered to be 1.5012 m before the structural vibration. System analysis under seismic excitations of this research showed that the maximum amplitude of displacement of the liquid in the vertical column is about 40 centimeters (as shown in Fig. 10). Therefore, in designing the damper, it should be noted that the minimum total height of the vertical column of the damper is more than two meters.

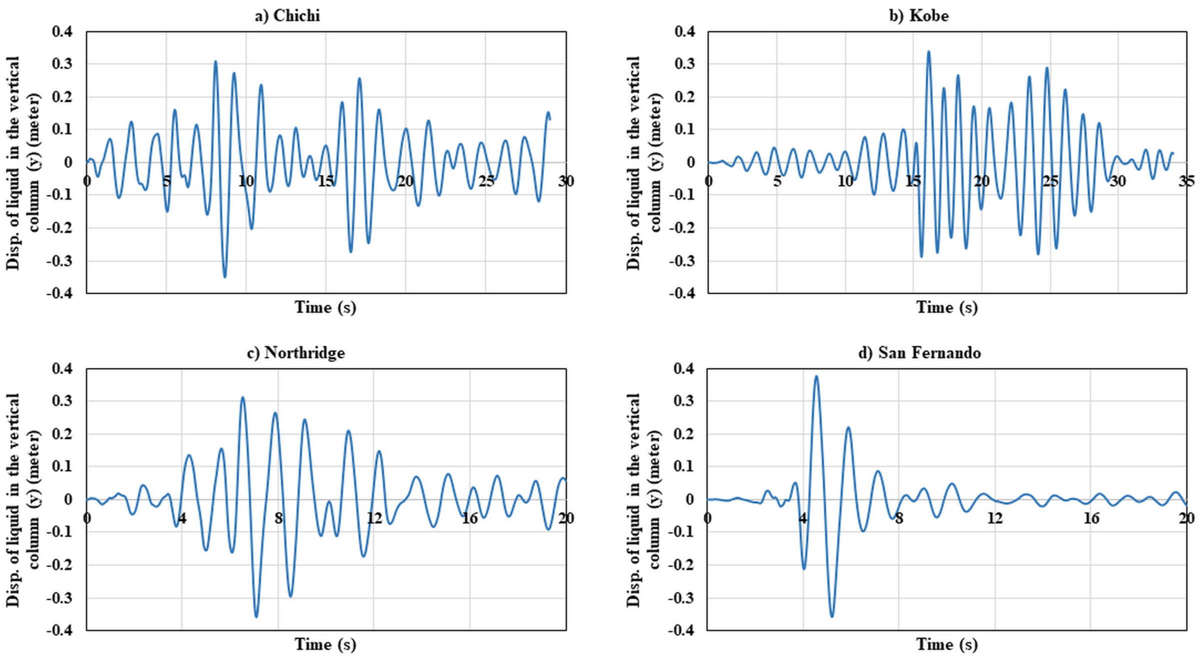

Fig. 10. Time history diagram of the displacement of the liquid in the vertical column (y)

7. Conclusion

This study was conducted using a semi-active liquid column gas damper (SALCGD) aimed at reducing the vibrations of the pile-supported wharf under earthquake load. Also, the optimal valve blocking rates of the horizontal column of the damper were obtained under 20 different earthquake loadings for the first time to use the maximum capacity of the SALCGD. The main results of this study are listed below:

- The optimal valve shut-off rate of the damper horizontal column was obtained as about 35%, which corresponds to a hydraulic loss factor of 5.
- On average, in different types of the pile-supported wharf, use of the SALCGD reduces the location of the deck of the berth as about 35%, while the passive TLCGD function has reduced the response of the structural movement by about 20%. It follows that the semi-activation of the damper will result in improved controlling function over the structure.
- It was also observed that the SALCGD also functions properly in reducing the acceleration of the structure, and consequently, reducing the shear forces applied to the system. Hence, the use of SALCGD reduces the response of the acceleration of the structure up to 50% compared to the uncontrolled mode and about 30% than to the passive control mode by the TLCGD.

Conflict of Interest

The author declared no potential conflicts of interest with respect to the research, authorship and publication of this article.

Funding

The author acknowledges the funding support of Babol Noshirvani University of Technology through Grant program No. BNUT/394097/98.

References

[1] Gerolymos, N., Giannakou, A., Anastasopoulos, I. and Gazetas, G., Evidence of beneficial role of inclined piles: observations and summary of numerical analyses. *Bulletin of Earthquake Engineering*, 6(4), 2008, 705-722.
[2] Poulos, H.G., Raked piles—Virtues and drawbacks. *Journal of Geotechnical and Geoenvironmental Engineering*, 132(6), 2006, 795-803.
[3] Oyenuga, D., Abrahamson, E., Krimotat, A., Kozak, A., Labasco, T. and Lobedan, F., A study of the pile-wharf deck connection at the Port of Oakland. In *Ports' 01: America's Ports: Gateway to the Global Economy*, 2001, 1-10.
[4] Mageau, D. and Chin, K., Effectiveness of stone columns on slope deformations beneath wharves. In *TCLEE 2009: Lifeline Earthquake Engineering in a Multihazard Environment,* 2009, 1-12.
[5] Soong, T.T. and Dargush, G.F., Passive Energy Dissipation Systems in Structural Engineering Wiley. *Chichester, UK*, 1997.
[6] Tributsch, A. and Adam, C., Evaluation and analytical approximation of Tuned Mass Damper performance in an earthquake environment. *Smart Structures and Systems*, 10(2), 2012, 155-179.
[7] De Domenico, D. and Ricciardi, G., Earthquake-resilient design of base isolated buildings with TMD at basement: Application to a case study. *Soil Dynamics and Earthquake Engineering*, 113, 2018, 503-521.
[8] De Domenico, D. and Ricciardi, G., Optimal design and seismic performance of tuned mass damper inerter (TMDI) for structures with nonlinear base isolation systems. *Earthquake Engineering & Structural Dynamics*, 47(12), 2018, 2539-2560.
[9] Elias, S., Matsagar, V. and Datta, T.K., Along-wind response control of chimneys with distributed multiple tuned mass dampers. *Structural Control and Health Monitoring*, 26(1), 2019, 2275.
[10] Nishimura, I., Kobori, T., Sakamoto, M., Koshika, N., Sasaki, K. and Ohrui, S., Active tuned mass damper. *Smart Materials and Structures*, 1(4), 1992, 306.
[11] Suleman, A., Oliveira, F., Botto, M. and Morais, P., Semi-active viscous damper for controlling civil engineering structures subjected to earthquakes. In *CONTROLO,* 2012.
[12] Di Matteo, A., Furtmüller, T., Adam, C. and Pirrotta, A., Optimal design of tuned liquid column dampers for seismic response control of base-isolated structures. *Acta Mechanica*, 229(2), 2018, 437-454.
[13] Min, K.W., Kim, H.S., Lee, S.H., Kim, H. and Ahn, S.K., Performance evaluation of tuned liquid column dampers for response control of a 76-story benchmark building. *Engineering Structures*, 27(7), 2005, 1101-1112.
[14] Di Matteo, A., Pirrotta, A. and Tumminelli, S., Combining TMD and TLCD: analytical and experimental studies. *Journal of Wind Engineering and Industrial Aerodynamics*, 167, 2017, 101-113.
[15] Hitchcock, P.A., Kwok, K.C.S., Watkins, R.D. and Samali, B., Characteristics of liquid column vibration absorbers (LCVA)—I. *Engineering Structures*, 19(2), 1997, 126-134.
[16] Hitchcock, P.A., Kwok, K.C.S., Watkins, R.D. and Samali, B., Characteristics of liquid column vibration absorbers (LCVA)—II. *Engineering Structures*, 19(2), 1997, 135-144.
[17] Yalla, S.K., Kareem, A. and Kantor, J.C., Semi-active tuned liquid column dampers for vibration control of structures. *Engineering Structures*, 23(11), 2001, 1469-1479.
[18] Hemmati, A. and Oterkus, E., Semi-Active Structural Control of Offshore Wind Turbines Considering Damage Development. *Journal of Marine Science and Engineering*, 6(3), 2018, 102.
[19] Hemmati, A., Oterkus, E. and Khorasanchi, M., Vibration suppression of offshore wind turbine foundations using tuned liquid column dampers and tuned mass dampers. *Ocean Engineering*, 172, 2019, 286-295.
[20] Hochrainer, M.J. and Ziegler, F., Control of tall building vibrations by sealed tuned liquid column

dampers. *Structural Control and Health Monitoring: The Official Journal of the International Association for Structural Control and Monitoring and of the European Association for the Control of Structures*, 13(6), 2006, 980-1002.
[21] Dezvareh, R., Bargi, K. and Mousavi, S.A., Control of wind/wave-induced vibrations of jacket-type offshore wind turbines through tuned liquid column gas dampers. *Structure and Infrastructure Engineering*, 12(3), 2016, 312-326.
[22] Bargi, K., Dezvareh, R. and Mousavi, S.A., Contribution of tuned liquid column gas dampers to the performance of offshore wind turbines under wind, wave, and seismic excitations. *Earthquake Engineering and Engineering Vibration*, 15(3), 2016, 551-561.
[23] Lindner-Silwester, T. and Schneider, W., The moving contact line with weak viscosity effects–an application and evaluation of Shikhmurzaev's model. *Acta Mechanica*, 176(3-4), 2005, 245-258.
[24] Cheng, F.Y., Jiang, H. and Lou, K., *Smart structures: innovative systems for seismic response control*. CRC Press, 2008.
[25] Mousavi, S.A., Bargi, K. and Zahrai, S.M., Optimum parameters of tuned liquid column–gas damper for mitigation of seismic-induced vibrations of offshore jacket platforms. *Structural Control and Health Monitoring*, 20(3), 2013, 422-444.
[26] Wu, J.C., Experimental calibration and head loss prediction of tuned liquid column damper. *Tamkang Journal of Science and Engineering*, 8(4), 2005, 319-325.
[27] Uang, C.M. and Bertero, V.V., *Use of energy as a design criterion in earthquake-resistant design,* Berkeley, California: Earthquake Engineering Research Center, University of California, 88(18), 1998.
[28] Sorace, S. and Terenzi, G., Seismic protection of frame structures by fluid viscous damped braces. *Journal of Structural Engineering*, 134(1), 2008, 45-55.
[29] De Domenico, D. and Ricciardi, G., Earthquake protection of structures with nonlinear viscous dampers optimized through an energy-based stochastic approach. *Engineering Structures*, 179, 2019, 523-539.
[30] Reggio, A. and Angelis, M.D., Optimal energy-based seismic design of non-conventional Tuned Mass Damper (TMD) implemented via inter-story isolation. *Earthquake Engineering & Structural Dynamics*, 44(10), 2015, 1623-1642.
[31] Towhata, I., Alam, M.J., Honda, T. and Tamate, S., Model tests on behaviour of gravity-type quay walls subjected to strong shaking. *Bulletin of the New Zealand Society for Earthquake Engineering*, 42(1), 2009, 47.
[32] Overseas coastal area development institute of Japan, Ports and harbours bureau, Ministry of land, infrastructure, transport and tourism, National institute for land and infrastructure management and Port and airport research institute, *Technical standards and commentaries for port and harbour facilities in Japan*. Overseas Coastal Area Development Institute of Japan, 2009.
[33] MATLAB, User Guide, Simulink, MathWorks Inc., Version 8.1.0, 2013.
[34] DeVries, P.L. and Hasbun, J.E., *A first course in computational physics*. Jones & Bartlett Publishers, 2011.
[35] Chopra, A.K. and Chopra, A.K., *Dynamics of structures: theory and applications to earthquake engineering,* Upper Saddle River, NJ: Pearson/Prentice Hall, 2007.
[36] PEER, Strong Ground Motion Database,http://peer.berkeley.edu/smcat/, 2009.
[37] ASCE7-10, Minimum Design Loads for Buildings and Other Structures, American Society of Civil Engineers (ASCE), Reston, Virginia, 2010.
[38] Wang, J.F., Lin, C.C. and Lian, C.H., Two-stage optimum design of tuned mass dampers with consideration of stroke. *Structural Control and Health Monitoring: The Official Journal of the International Association for Structural Control and Monitoring and of the European Association for the Control of Structures*, 16(1), 2009, 55-72.